CHAPTER IV
RESULTS AND DISCUSSION

4.1 Characterization of Chitosan

4.1.1 Structural Characterization

Chitosan obtained was characterized by using FTIR. The FTIR spectrum of chitosan was shown in Figure 4.1. The main characteristic peaks of chitosan are at 3450 (O-H stretching), 2876 (C-H stretching), 1594 (N-H bending), 1154 (bridge O stretching), and 1093 (C-O stretching).

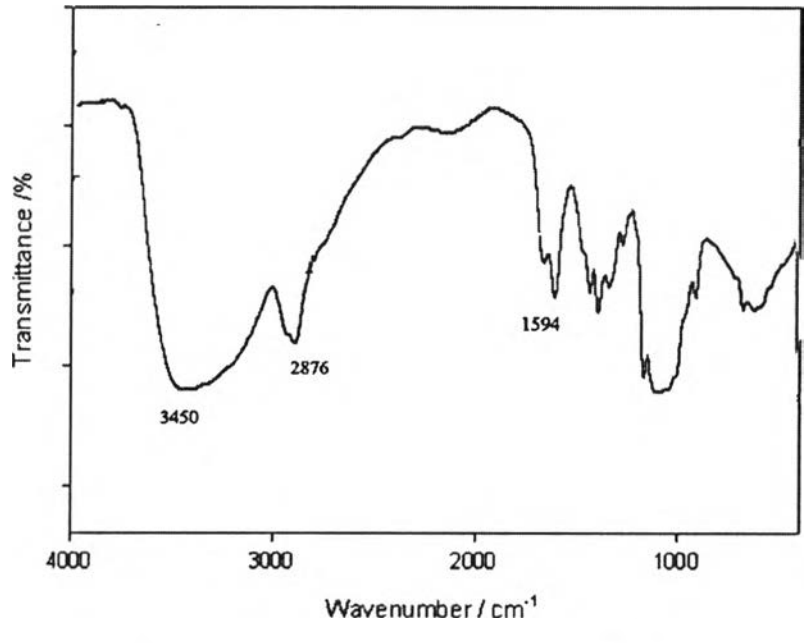

Figure 4.1 FTIR spectrum of chitosan.

4.1.2 Degree of Deacetylation

The degree of deacetylation of chitosan was confirmed by infrared spectroscopic measurement according to the method of Baxter *et al.*, (1992). The value obtained was 97%.

4.1.3 Viscosity-Average Molecular weight

The molecular weights of chitosan were determined by using the intrinsic viscosity method. The molecular weight of chitosan was about 422,240.

4.2 Characterization of *O*-CM chitosan

4.2.1 Structural Characterization

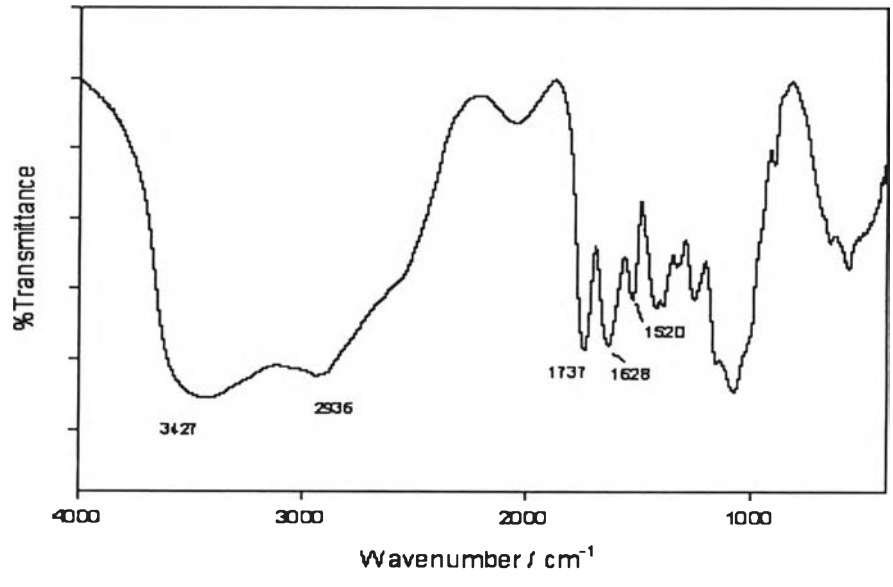

Figure 4.2 FTIR spectrum of H-form of *O*-CM chitosan.

Figure 4.2 shows FTIR spectrum of *O*-CM chitosan. The absorption frequencies of characteristic bands of *O*-CM chitosan were observed at 1737 cm^{-1} (-COOH), 1628 and 1520 cm^{-1} ($-NH_3^+$).

4.2.2 Degree of Substitution

The degree substitution of O-CM chitosan was about 1.0. (i.e. Calcd. C 38.50 H 5.23 N 5.57; Found C 38.35 H 5.52 N 5.56).

4.3 Characterization of *N*-(carboxyacyl) chitosan

4.3.1 Structural Characterization

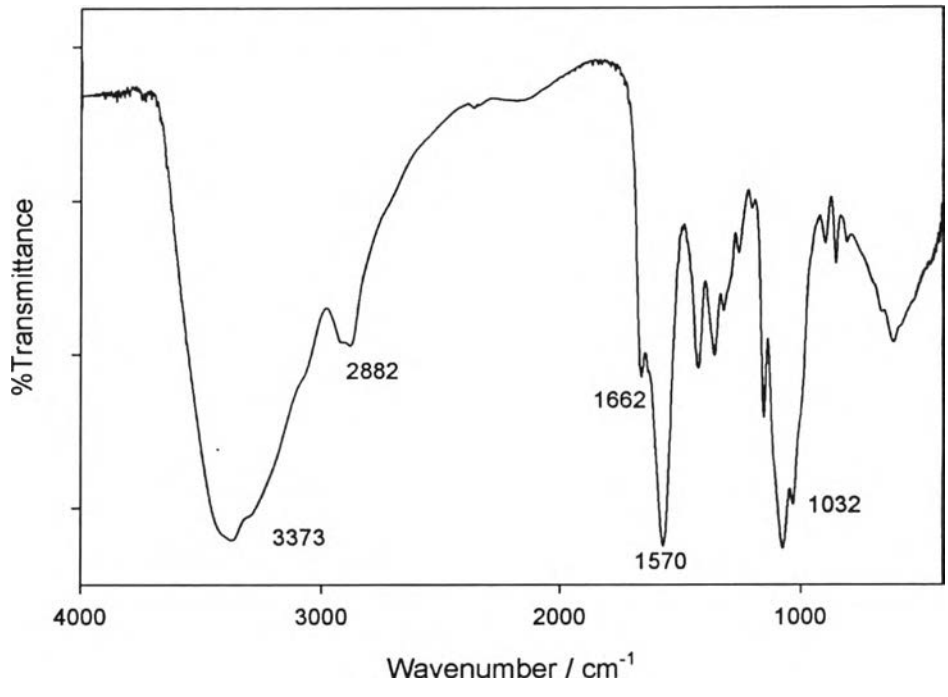

Figure 4.3 FTIR spectrum of *N*-(carboxyacyl) chitosan.

Figure 4.3 shows FTIR spectra of *N*-(carboxyacyl) chitosan , *N*-(3'-carboxypropen-2'-oyl) chitosan obtained by reacting with maleic anhydride, shows the characteristic absorption bands at 1662 and 1570 cm^{-1} which assigned to C=O stretching and N-H bending of *N*-acyl group

4.3.2 Degree of Substitution

The degree of substitution calculated on the basis of C/N ratio in the elemental analysis was about 0.48.

4.4 Characterization of Sodium Alginate

4.4.1 Structural Characterization

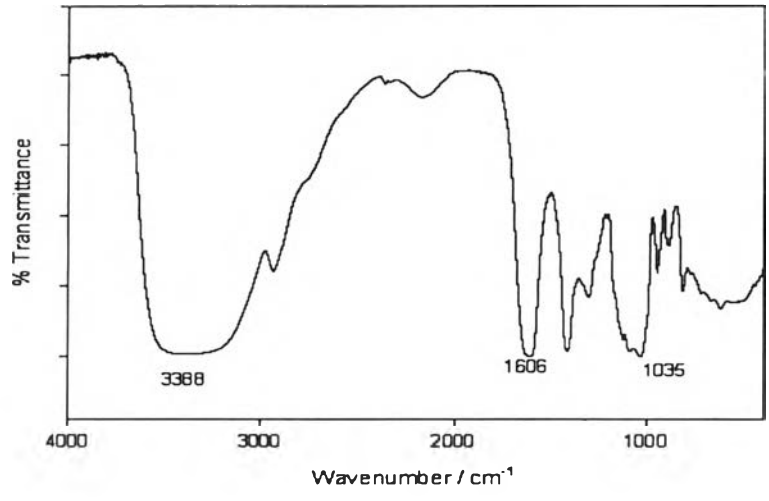

Figure 4.4 FTIR spectrum of alginate.

Figure 4.4 shows FTIR spectrum of alginate. The absorption frequencies of characteristic bands of alginate were observed at 3388(O-H stretching), 1606 (C=O stretching), and 1035 (C-O-C stretching).

4.4.2 Viscosity-Average Molecular Weight

The molecular weights of alginate was determined by using the intrinsic viscosity method. The molecular weight of alginate was calculated to be 318,203.

4.5 Characterization of Blend Film

4.5.1 Interaction in *O*-CM chitosan/Alginate Blend Film

The FTIR spectra of alginate, *O*-CM chitosan and *O*-CM chitosan/alginate blend films with 0.5%, 1.0%, and 1.5% *O*-CM chitosanl contents are shown in Figure 4.5. The FTIR spectra of pure alginate shows the characteristic absorption bands at 3388, 1605, and 1035 cm^{-1} which assigned to –OH stretching,

C=O stretching, and C-O-C stretching, respectively. For pure *O*-CM chitosan, the characteristic absorption bands were observed at 1600 cm^{-1} (C=O stretching of -O-CO-CH_3). In the blend, the –OH stretching vibration bands were broadened and the absorption band at 1605 cm^{-1} of pure alginate was shifted to higher wavenumber at around 1630 cm^{-1} , suggesting that intermolecular hydrogen bonds involving hydroxyl groups exist in the blend films. Moreover, all the blend films have a new absorption band at 1732 cm^{-1} caused by electrostatic interaction between -COOH groups of alginic acid and $-NH_2$ groups of *O*-CM chitosan. The FTIR results indicated that the blend between the two kinds of molecules is miscible, due to the strong electrostatic force and intermolecular hydrogen bonding.

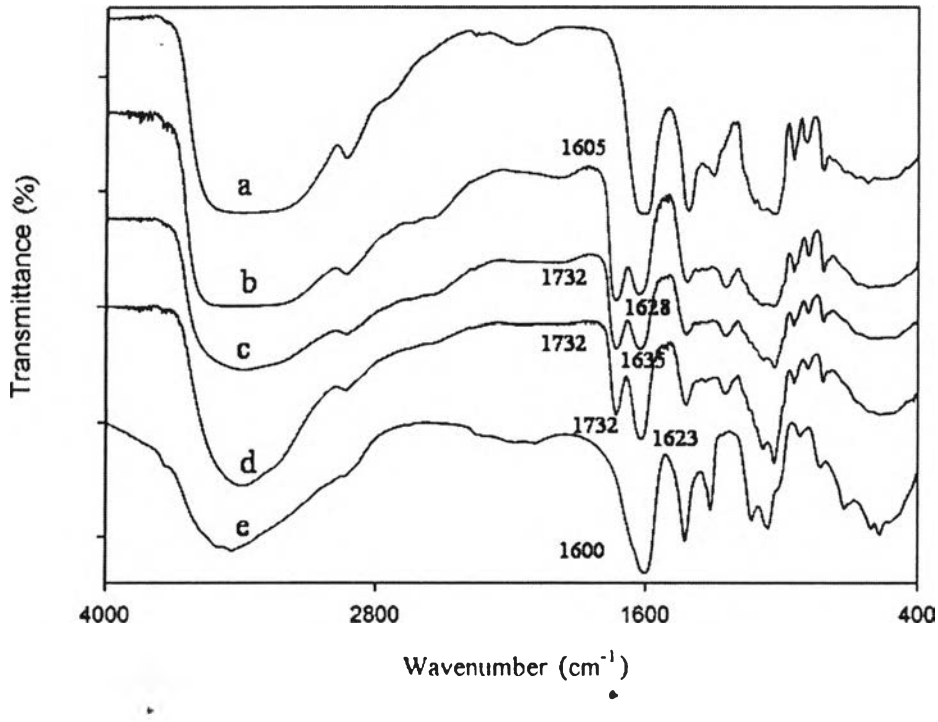

Figure 4.5 FTIR spectra of (a) alginate film, *O*-CM chitosan/alginate blend films with (b) 0.5%, (c) 1.0% and (d) 1.5% *O*-CM chitosan contents,
(e) *O*-CM chitosan film.

4.5.2 Interaction in *N*-(carboxyacyl) chitosan(*N*-CA)/Alginate Blend Film

The FTIR spectra of *N*-(carboxyacyl) chitosan , *N*-(3'-carboxypropen-2'-oyl) chitosan obtained by reacting with maleic anhydride, shows the characteristic absorption bands at 1662 and 1570 cm^{-1} which assigned to C=O stretching and N-H bending of *N*-acyl group. In the blend, the –OH stretching vibration bands were broadened and the absorption band at 1605 cm^{-1} of pure alginate was shifted to higher wavenumber at around 1623 cm^{-1} , suggesting that intermolecular hydrogen bonds involving hydroxyl groups exist in the blend films (Figure 4.6). Moreover, all the blend films have a new absorption band at 1732 cm^{-1} caused by electrostatic interaction between -COOH groups of alginic acid and $-NH_2$ groups of *N*-(carboxyacyl) chitosan. The FTIR results indicated that the blend between alginate and *N*-(carboxyacyl) chitosan was miscible for all blend compositions similar to *O*-CM chitosan/alginate blend films.

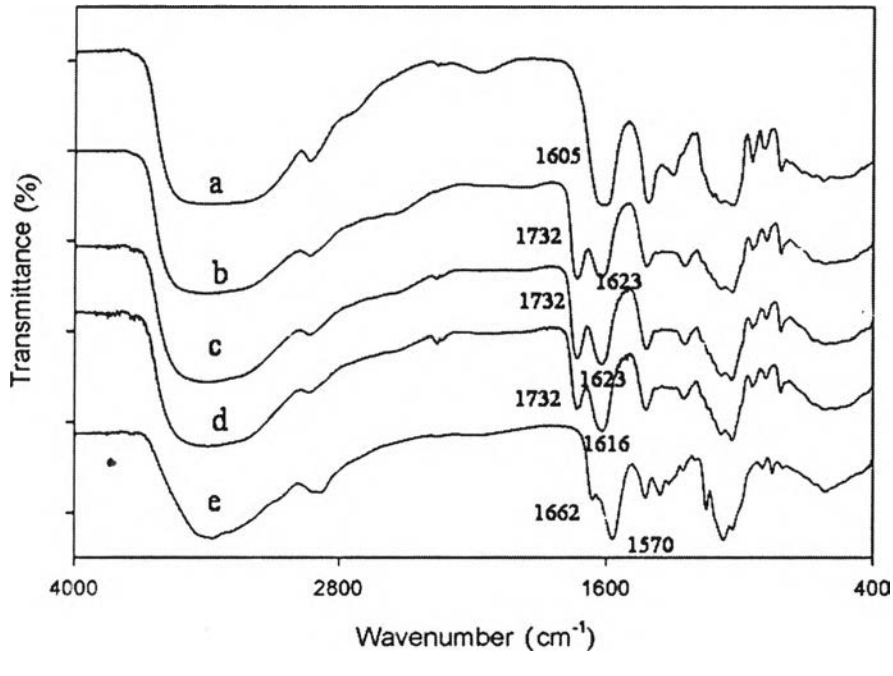

Figure 4.6 FTIR spectra of (a) alginate film, *N*-CA chitosan/alginate blend films with (b) 0.25%, (c) 0.50% and (d) 0.75% *N*-CA chitosan contents, (e) *N*-(carboxyacyl) chitosan film (*N*-CA chitosan).

4.6 Characterization of Blend Fiber

4.6.1 SEM Micrographs of *O*-CM chitosan/Alginate Blend Fiber

In this study, SEM was used to observe fiber surfaced. SEM micrographs of the blend fibers are shown in Figure 4.7. It was found that there was no remarkable change on fiber surface morphology among the different *O*-CM chitosan1 contents in spinning dopes studied in this work.

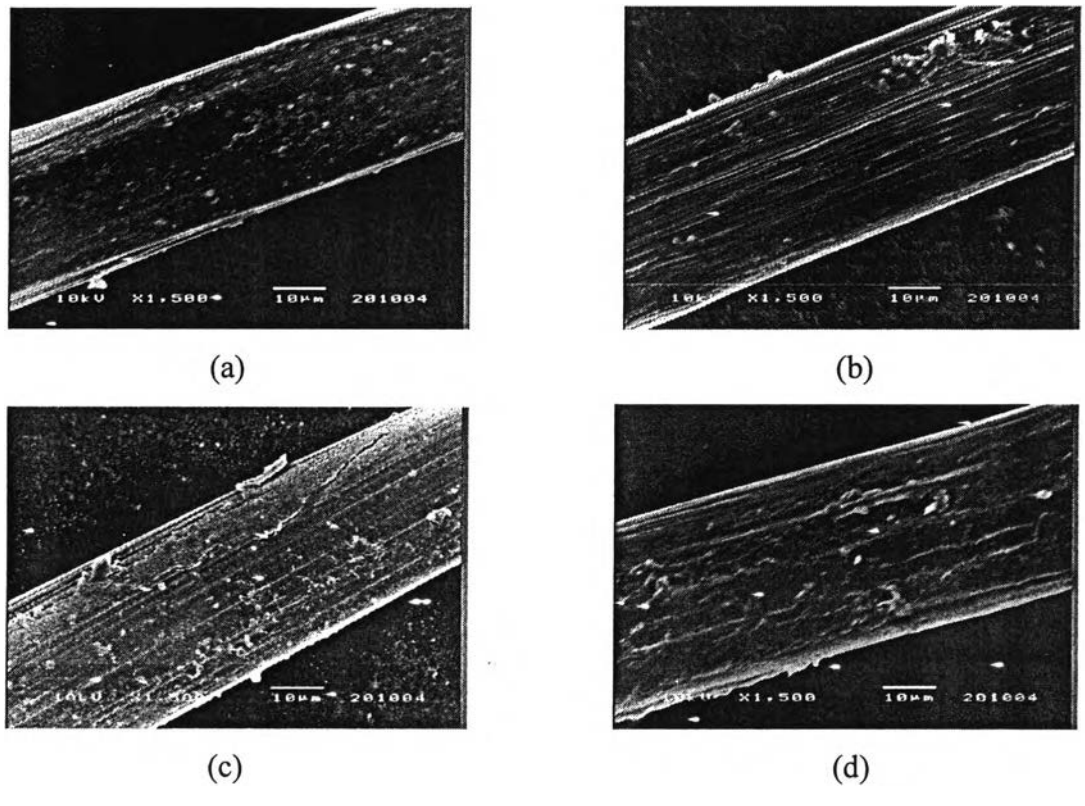

Figure 4.7 SEM micrographs of (a) alginate fiber, (b) 0.5% *O*-CM chitosan/alginate blend fiber, (c) 1.0% *O*-CM chitosan/alginate blend fiber and (d) 1.5% *O*-CM chitosan/alginate blend fiber.

4.6.2 SEM Micrographs of *N*-(carboxyacyl) chitosan/Alginate Blend Fiber

SEM micrographs of the blend fibers are shown in Figure 4.8. It was found that there was no remarkable change on fiber surface morphology among the different *N*-(carboxyacyl) chitosan contents.

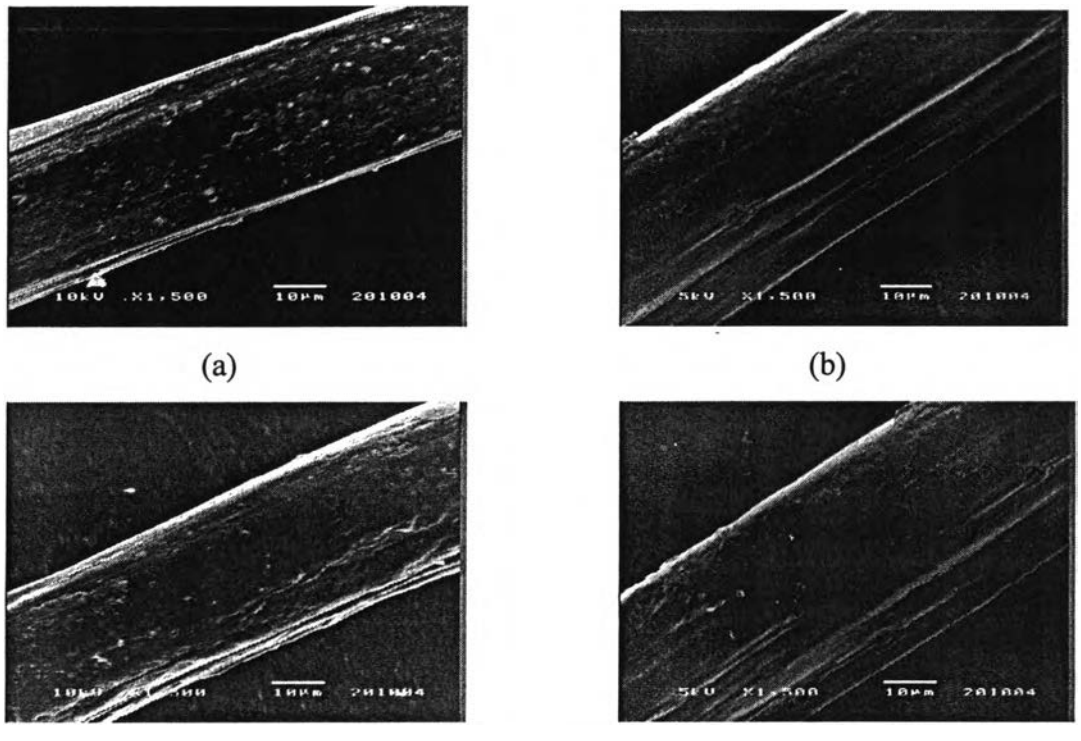

Figure 4.8 SEM micrographs of (a) alginate fiber, (b) 0.25% *N*-(carboxyacyl) chitosan /alginate blend fiber, (c) 0.50% *N*-(carboxyacyl) chitosan /alginate blend fiber and (d) 0.75% *N*-(carboxyacyl) chitosan /alginate blend fiber.

4.6.3 DSC Analysis of *O*-CM chitosan/Alginate Blend Fiber

The thermal transitions of alginate, *O*-CM chitosan, and the blend fibers were determined by DSC analysis (Figure 4.9). Due to a certain amount of free water containing in the samples, all spectra give a significant transition at about 100°C except *O*-CM chitosan. The identification of this transition peak implied the good moisture-retention of alginate was not affected by addition of *O*-CM chitosan similar to the result obtained from chitosan/*N,O*-carboxymethylated chitosan/viscose

rayon fibers from the previous study. The single endothermic peak in range of 200-240 °C suggested that some chain scission and loss of water molecules coming from the primary –OH groups of alginate in the fibers. Interestingly, an exothermic peak of the *O*-CM chitosan appears at 274°C, owing to the decomposition of *O*-CM chitosan, but this peak disappears in DSC thermograph of the blend fibers. The result supported the conclusion on the miscibility of the blends.

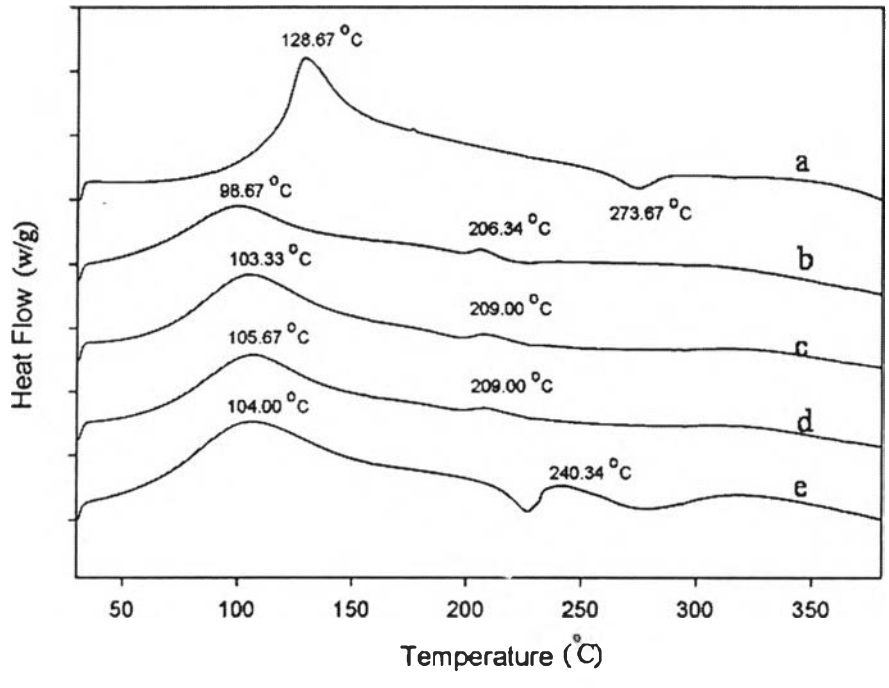

Figure 4.9 DSC spectra of (a) *O*-CM chitosan powder, *O*-CM chitosan/alginate blend fibers with (b) 0.5%, (c) 1.0% and (d) 1.5% *O*-CM chitosan contents, (e) alginate fiber.

4.6.4 DSC Analysis of *N*-(carboxyacyl) chitosan/Alginate Blend Fiber

The result of *N*-(carboxyacyl) chitosan/alginate blend fiber in Figure 4.10 is similar to *O*-CM chitosan/alginate blend fiber. The result supports the conclusion on the miscibility of the blends.

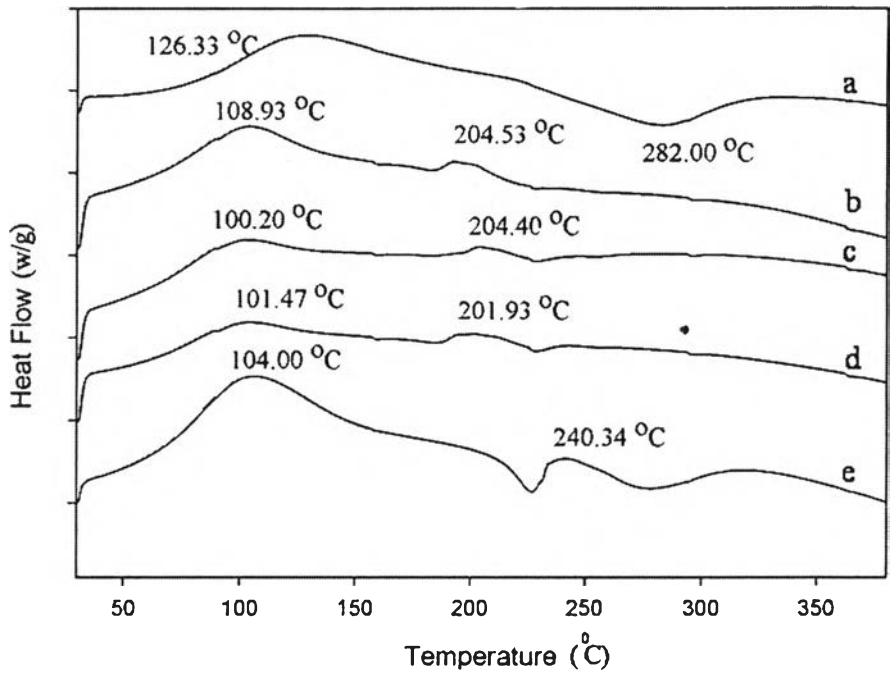

Figure 4.10 DSC spectra of (a) *N*-(carboxyacyl) chitosan powder (*N*-CA), *N*-CA chitosan/alginate blend fibers with (b) 0.25%, (c) 0.50% and (d) 0.75% *N*-CA chitosan contents, (e) alginate fiber.

4.6.5 Wide-angle X-ray Analysis of *O*-CM chitosan/Alginate Blend Fiber

X-ray scattering patterns of *O*-CM chitosan, alginate fiber and blend fibers are shown in Figure 7. There is a strong peak in the diffractogram of *O*-CM chitosan powder at 2θ being 32° indicating the high crystallinity of *O*-CM chitosan powder. The diffractogram of the blend fiber reveals that crystallinity of the blend fibers was lower than that of alginate fiber. No peak found at around 2θ = 32° in the diffractograms of blend fibers. This indicated that the *O*-CM chitosan did not form its own crystalline region in the blends and maintained amorphous state during fiber formation. The results were the same as the previous work of *O*-carboxymethylated chitosan/cellulose blend film from LiCl/*N,N*-dimethylacetamide solution.

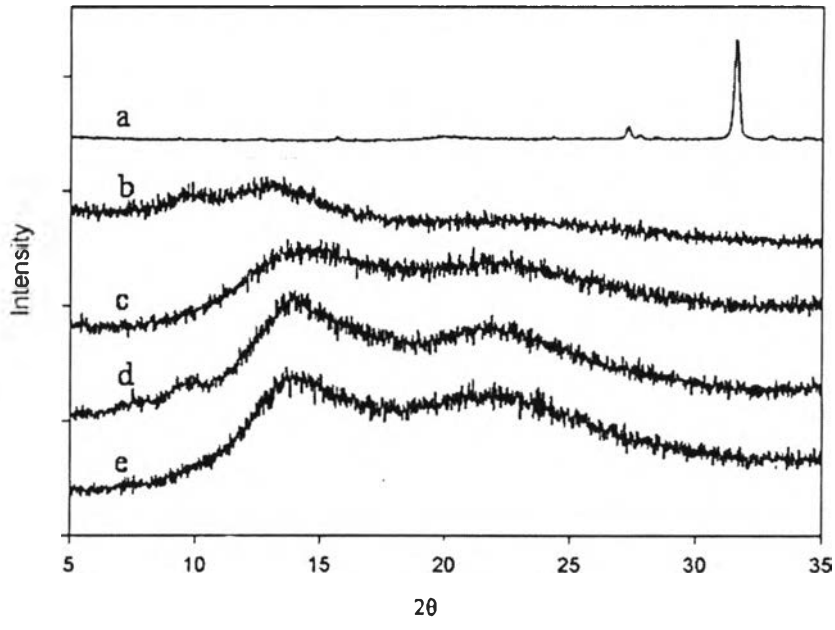

Figure 4.11 XRD spectra of (a) *O*-CM chitosan powder, (b) alginate fiber, *O*-CM chitosan/alginate blend fibers with (c) 0.5%, (d) 1.0% and (e) 1.5% *O*-CM chitosan contents.

4.6.6 Wide-angle X-ray Analysis of *N*-(carboxyacyl) chitosan/Alginate Blend Fiber

X-ray scattering patterns of *N*-(carboxyacyl) chitosan, alginate fiber and the blend fibers are shown in Figure 4.12. The diffractogram of the blend fiber reveals that crystallinity of the blend fibers was lower than that of alginate fiber. The result was similar to *O*-CM chitosan/alginate blend fiber.

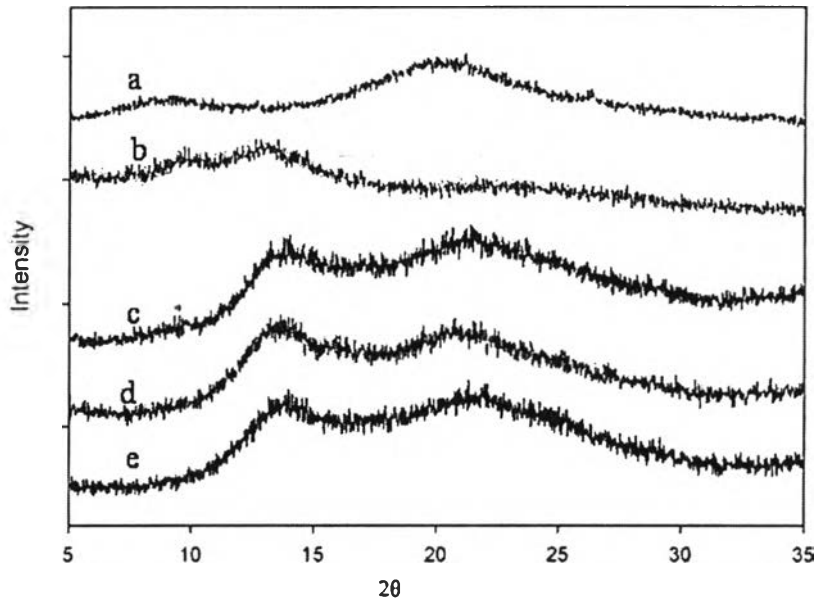

Figure 4.12 XRD spectra of (a) *N*-(carboxyacyl) chitosan powder (*N*-CA chitosan), (b) alginate fiber, *N*-CA chitosan/alginate blend fibers with (c) 0.25%, (d) 0.50% and (e) 0.75% *N*-CA chitosan contents.

4.6.7 Calcium Content in The Blend Fiber

Table 4.1 shows the calcium contents in the pure alginate fiber and in *O*-CM chitosan/alginate blend fibers. The calcium contents in the blend fibers were lower than that in the pure alginate fiber due to the amount of alginate in the blend fibers was decreased. Furthermore, when *O*-CM chitosan contents in the blend fibers increased, the calcium content in the blend fibers decreased due to *O*-CM chitosan disrupted the interaction between alginate molecules and calcium ions during the spinning process

Similar to *O*-CM chitosan/alginate blend fiber, the calcium contents in the *N*-(carboxyacyl) chitosan/alginate blend fibers were lower than that in the pure alginate fiber and lower also than that of *O*-CM chitosan/alginate blend fiber at the same concentration.

Table 4.1 Calcium content in alginate and the blend fibers
([a] average values form three experiments)

Fiber	Calcium content (mg/100g fiber)[a]
Pure alginate fiber	6853.28
0.50% O-CM chitosan/alginate blend fiber	3568.77
1.00% O-CM chitosan/alginate blend fiber	2390.44
1.50% O-CM chitosan/alginate blend fiber	2125.44
0.25% *N*-CA chitosan /alginate blend fiber	1869.16
0.50% *N*-CA chitosan /alginate blend fiber	1500.94
0.75% *N*-CA chitosan /alginate blend fiber	1375.46

4.6.8 Mechanical Properties of The Blend Fiber

Mechanical properties of *O*-CM chitosan/alginate blend fibers are summarized in Table 4.2. The tenacity and elongation of the blend fibers were lower than that of the pure alginate fiber and decreased with increasing of *O*-CM chitosan content. However, the tenacity of the blend fibers was slightly decreased as increasing of *O*-CM chitosan content.

For *N*-(carboxyacyl) chitosan /alginate blend fiber, the tenacity and elongation of the blend fibers were remarkably lower than that of the pure alginate fiber. The tenacity of the blend fibers was decreased as increasing of *N*-(carboxyacyl) chitosan content but slightly lower than that of *O*-CM chitosan/alginate blend fiber. It has been reported that the presence of chitosan limits the crystalline of cellulose. This may be attributed to the addition of chitosan derivatives, which slightly hamper the crystallization of alginate molecules during the spinning process. However, in the present study, it is interesting to find that the tenacity of the blend fibers almost approach to that of original alginate fiber.

Table 4.2 Mechanical properties of alginate and the blend fibers
([a]average values of twenty fiber samples)

Fiber	Tenacity (cN/tex)[a]	Elongation at break(%)[a]
Pure alginate fiber	12.53 ±1.05	15.65 ±1.96
0.50% O-CM chitosan/alginate blend fiber	12.16 ± 0.91	9.03 ± 1.20
1.00% O-CM chitosan/alginate blend fiber	12.02 ± 1.61	11.02 ±1.96
1.50% O-CM chitosan/alginate blend fiber	11.98 ± 1.10	11.08 ± 1.38
0.25% *N*-CA chitosan/alginate blend fiber	10.42 ± 1.22	10.63 ± 0.86
0.50% *N*-CA chitosan/alginate blend fiber	9.90 ± 0.56	10.36 ± 1.19
0.75% *N*-CA chitosan/alginate blend fiber	9.62 ± 0.85	13.16 ± 1.88

4.6.9 Antimicrobial Properties of The Blend Fiber

Antimicrobial activities of *O*-CM chitosan/alginate blend fibers against gram-negative bacteria (*Escherichia coli*, *Pseudomonas auruginosa*), gram-positive bacteria (*Staphylococcus aureus*, *Staphylococcus mutans*), and yeasts (*Saccharomyces cerevisiae*, *Candida albicans*) of the blend fibers were qualitatively investigated by observing the clear zones between the fibers and luxuriant bacteria colonies and the results were shown in Table 4.3.

The blend fibers with about 170 mg. of each sample and the fiber area about 1.5 cm. × 4 cm were prepared. The *O*-CM chitosan contents in the tested 0.5%, 1.0%, and 1.5% *O*-CM chitosan/alginate blend fibers were 13.07, 24.29 and 34 mg, respectively. The clear zone surrounding the tested fibers was evidence that the *O*-CM chitosan/alginate blend fibers could inhibit the growth of *E .coli*, *P. aureginosa, S. aureus*, *S. mutans* and *S. cerevisiae* except *Candida albicans*..

Similar to *O*-CM chitosan/alginate blend fiber, *N*-(carboxyacyl) chitosan contents in the tested 0.25%, 0.50%, and 0.75% *N*-(carboxyacyl) chitosan/alginate blend fibers were about 6.8, 13.07, and 18.89 mg, respectively.

The clear zone surrounding the tested fibers was evidence that the *N*-(carboxyacyl) chitosan/alginate blend fibers could inhibit the growth of *E .coli*, *P. aureginosa, S. aureus*, *S. mutans* and *S. cerevisiae* except *Candida albicans.* similar to *O*-CM chitosan/alginate blend fibers. The reason may be due to the chitosan derivative content was lower than the minimum inhibitory concentration of *Candida Albicans.*

Interestingly, the clear zones of *N*-(carboxyacyl) chitosan/alginate blend fibers were quite larger than those of *O*-CM chitosan/alginate blend fibers at the same chitosan derivative content. The results indicated that the chitosan derivative/alginate blend fibers would be suitable to be used as wound dressing with antimicrobial properties.

Table 4.3 Effect of alginate-based antimicrobial fibers on inhibition zone area against microorganisms; $+^{W}$: Inhibition is weak (clear zone is <0.5 mm), +: clear zone is 0.5-2.0 mm, ++ : clear zone is 2.0-4.0 mm, $++^{S}$: Inhibition is strong clear zone is >4 mm), -: no antimicrobial

Alginate-based fibers	Microorganism					
	E. coli	*P. aureginosa*	*S. aureus*	*S. mutans*	*Candida albicans*	*S. cerevisiae*
Pure alginate fiber	-	-	-	-	-	-
0.5% *O*-CM chitosan	$+^{W}$	$+^{W}$	$+^{W}$	$+^{W}$	-	+
1.0% *O*-CM chitosan	+	+	+	+	-	+
1.5% *O*-CM chitosan	+	+	++	+	-	+
0.25% *N*-CA chitosan	+	$+^{W}$	+	+	-	++
0.50% *N*-CA chitosan	+	+	+	++	-	++
0.75% *N*-CA chitosan	++	+	+	++	-	++
0.1% triclosan	$++^{S}$	$++^{S}$	$++^{S}$	$++^{S}$	$++^{S}$	$++^{S}$